Journal of Theoretical Biology 253 (2008) 228–237

Contents lists available at ScienceDirect

Journal of Theoretical Biology

journal homepage: www.elsevier.com/locate/yjtbi

The effect of superspreading on epidemic outbreak size distributions

T. Garske [a,b,*], C.J. Rhodes [a,b,1]

[a] Institute for Mathematical Sciences, Imperial College London, 53 Prince's Gate, Exhibition Road, South Kensington, London SW7 2PG, UK
[b] Infectious Disease Epidemiology Group, Imperial College London, Norfolk Place, London SW2 1PG, UK

ARTICLE INFO

Article history:
Received 5 June 2007
Received in revised form
29 February 2008
Accepted 29 February 2008
Available online 6 March 2008

Keywords:
Heterogeneous transmission
Epidemic model
Branching process
Vaccination

ABSTRACT

Recently, evidence has been presented to suggest that there are significant heterogeneities in the transmission of communicable diseases. Here, a stochastic simulation model of an epidemic process that allows for these heterogeneities is used to demonstrate the potentially considerable effect that heterogeneity of transmission will have on epidemic outbreak size distributions. Our simulation results agree well with approximations gained from the theory of branching processes. Outbreak size distributions have previously been used to infer basic epidemiological parameters. We show that if superspreading does occur then such distributions must be interpreted with care. The simulation results are discussed in relation to measles epidemics in isolated populations and in predominantly urban scenarios. The effect of three different disease control policies on outbreak size distributions are shown for varying levels of heterogeneity and disease control effort.

1. Introduction

Classical models for the spread of infectious diseases tend to assume that infected individuals are fairly homogeneous with respect to transmission (Anderson and May, 1991). By this, we mean that each infective has the same potential to transmit the pathogen as any other, and each susceptible is equally likely to contract the disease on contact with an infective. In contrast, in some applications, such as sexually transmitted diseases, these models have long been known to fail to reproduce the observed disease dynamics, which lead to the development of network models to account for differences in the number of partners thereby influencing the probability of contracting and transmitting the disease (Hethcote and Yorke, 1984; May and Anderson, 1987).

However, the number of diseases in which heterogeneity of transmission has been observed is ever growing, with examples ranging from macroparasitic infections, in which a large proportion of the parasite burden is carried by a small proportion of the population (Galvani, 2003; Grenfell et al., 1995), over livestock diseases such as the foot-and-mouth disease epidemic in the UK in 2001 (Ferguson et al., 2001; Woolhouse et al., 2005), or patterns of *Escherichia coli* infection in cattle (Matthews et al., 2006) to the SARS epidemic in 2003 (Chen et al., 2006; Lipsitch et al., 2003).

These observations have led to the formulation of the 80/20 rule, according to which in many diseases more than 80% of transmissions are causes by the most infectious 20% of cases (Woolhouse et al., 1997). These differences between infective cases can have an impact on disease dynamics and effectiveness of control strategies (Matthews and Woolhouse, 2005). Some situations like sexually transmitted diseases and livestock diseases (spread by animal movements between farms) are appropriately described by network models (Kiss et al., 2006; Truscott et al., 2007). These models take account of mixing patterns in the population because "superspreaders" (i.e., individuals that cause unusually many transmissions) are more likely to transmit to other superspreaders (consider for instance sex-workers and their clients) therefore forming a core group with much higher prevalence of disease than in the general population. However, the SARS epidemic has demonstrated that these correlations in infectiousness between parent- and daughter-cases do not always exist, calling for simpler models that nevertheless take account of the heterogeneity in transmission (James et al., 2007; Lloyd-Smith et al., 2005; Sguanci et al., 2006).

As the presence of superspreading appears to be a relatively common phenomenon both in established and emerging diseases, it is of interest to investigate the impact that superspreading might have on diseases dynamics in various contexts. Here, we concentrate on the patterns of disease outbreaks occurring in populations that are subject to the occasional introduction of disease by an index case. In practice, this addresses situations where an individual in the population gets infected from contact

* Corresponding author at: Institute for Mathematical Sciences, Imperial College London, 53 Prince's Gate, Exhibition Road, South Kensington, London SW7 2PG, UK. Tel.: +44 20 594 0967.
E-mail addresses: t.garske@imperial.ac.uk (T. Garske), c.rhodes@imperial.ac.uk (C.J. Rhodes).
[1] Tel.: +44 20 594 1753.

0022-5193/$ - see front matter © 2008 Elsevier Ltd. All rights reserved.
doi:10.1016/j.jtbi.2008.02.038

with a reservoir (possible zoonotic) or situations where index cases travel into the community from outside. Specifically, the quantity we are most interested in is the distribution of epidemic outbreak sizes. This is a useful indicator of the status of a disease within a population (Farrington et al., 2003; Jansen and Stollenwerk, 2005; Jansen et al., 2003; Rhodes and Anderson, 1996; Rhodes et al., 1997; Trottier and Philippe, 2005) and can be used to give an indication of the likelihood of pandemic emergence, given a sequence of outbreak data in a given area. To do this, we use results from branching process theory and a stochastic simulation model that allows for superspreading.

We show that the presence of superspreading can have a significant impact of the pattern of disease outbreaks and that care must be taken in interpreting epidemiological data where the intention is to gain insight into parameters such as the basic reproductive number, R_0. The pattern of disease outbreaks in the presence of superspreading is discussed with reference to measles outbreaks in two different locations, and this suggests that heterogeneity may be connected with the different responses of the populations to the presence of disease. A further motivation for this analysis is the impact that superspreading might have on the design of intervention strategies, an issue emphasised by Lloyd-Smith et al. (2005). We investigate population-wide and individual-based control policies, and investigate under what circumstances which is the more advantageous policy. More specifically, in circumstances where control can be achieved (i.e., the mean reproductive number is reduced below the threshold value of 1), under a population-wide control policy the probability of large outbreaks is smaller than under individual-based control, whereas if controls fail to reduce the reproductive number below 1, the probability of stochastic extinction of the disease is higher under individual-based control.

Section 2 describes the basic modelling framework to be used in this study, with application to an SIR-type scenario. Some basic simulation and analytic results are presented. In Section 3 the model is extended to include birth/death processes in a finite population. The behaviour of this model is interpreted in the light of some epidemiological data from isolated island populations and from predominantly urban populations in the UK. Section 4 discusses the impact that heterogeneous disease transmission can have on the selection of effective disease control strategies. Detailed derivations and analytic details are presented in Appendices A and B.

2. Epidemiological model

In communicable disease modelling, the reproductive number of any infectious case is the number of secondary infections it creates. This number is determined by the intrinsic infectivity of a single case, and the environment in which a case exists, for instance, the number of susceptibles that it comes into contact with. The basic reproductive number R_0 is the number created by a typical infected individual introduced into an otherwise fully susceptible population. In classical epidemic models, it is usually assumed that individuals are identical with respect to their infectivity. Here, we relax this assumption and allow for individual differences in infectivity.

A stochastic Markov chain model in continuous time is used to simulate epidemics in a homogeneously mixing infinite population. This model is very similar to the one used by Lloyd-Smith et al. (2005). It differs in that they used a pure branching process with discrete generations, whereas our model is implemented in continuous time, therefore giving more realistic epidemic curves. However, most of the results shown here (particularly those concerning the outbreak sizes in an infinite population) are identical to what would have been obtained with the simpler branching process model.

Each individual case is characterised by its intrinsic infectivity, which is expressed as the expected reproductive number R_{exp}. There are principally two ways of achieving heterogeneity of the expected reproductive number:

(i) varying the infectiousness (i.e., the rate of transmission, given an unlimited supply of susceptibles) between cases;
(ii) keeping the infectiousness constant, but varying the duration of infectiousness.

Here, we follow the former approach. Note that in many conventional epidemic models that are based on rates of recovery rather than a fixed duration of infectiousness, the duration of infectiousness is exponentially distributed, thereby yielding a model with a moderate amount of heterogeneity in transmission (Anderson and May, 1991). Additionally, the mean R_{exp} is equivalent to the basic reproductive number R_0.

Disease transmission is assumed to follow a Poisson process, so the actually observed reproductive number R_{act} for this case is a random variable, distributed according to a Poisson distribution with mean R_{exp}. Therefore, for this case the probability of observing actual reproductive number R_{act} is given by

$$P(R_{\text{act}}; R_{\text{exp}}) = \frac{R_{\text{exp}}^{R_{\text{act}}}\, \mathrm{e}^{-R_{\text{exp}}}}{R_{\text{act}}!}. \tag{1}$$

When transmission is homogeneous, i.e., if all cases in the population have the same expected reproductive number (as is usually assumed in standard epidemic models), Eq. (1) also describes the offspring distribution (Harris, 1963), and gives the distribution of observed reproductive numbers over the whole epidemic. However, following Lloyd-Smith et al. (2005), we assume here that the individual reproductive numbers R_{exp} are heterogeneous across the epidemic, being distributed according to some probability density function $Q(R_{\text{exp}})$. Integrating over all possible expected reproductive numbers, the distribution of the actual reproductive numbers in an epidemic is then given by

$$P(R_{\text{act}}) = \int P(R_{\text{act}}; R_{\text{exp}}) Q(R_{\text{exp}})\, \mathrm{d}R_{\text{exp}}. \tag{2}$$

While the distribution of expected reproductive numbers $Q(R_{\text{exp}})$ is necessary for the implementation of the continuous-time model, the outbreak size distributions we are primarily interested in are identical to those of a Galton–Watson branching process with the same offspring distribution $P(R_{\text{act}})$. In order to investigate the effects of superspreading, we need to consider an offspring distribution that can produce a variety of shapes ranging from well localised to strongly over-dispersed. A family of possible distributions are the power-series offspring distributions used by Becker (1974), given by

$$P(R_{\text{act}}) = \frac{a(R_{\text{act}})\theta^{R_{\text{act}}}}{A(\theta)}, \tag{3}$$

where $A(\theta) = \sum a(R_{\text{act}})\theta^{R_{\text{act}}}$.

Using branching process theory, it is possible to calculate the mean outbreak size, and approximate the outbreak size distribution in the limit of large outbreak sizes (Harris, 1963; Otter, 1949). While the mean outbreak size depends only on the basic reproductive number R_0 (i.e., the mean of the offspring distribution), for any offspring distribution (Haccou et al., 2005), see also Appendix A, this is not the case for the distribution of outbreak sizes. Defining $P(s)$ to be the probability of observing an outbreak of size s, then

$$P(s) \approx B^{1/2}\alpha^{-s}s^{-3/2}. \tag{4}$$

This approximation holds exact in the limit of large outbreak sizes. α and B depend on the particular form of the offspring distribution.

Here, we use a subset of the power-series offspring distribution for which the underlying distribution of expected reproductive numbers is known and which covers a wide variety of shapes. Following Lloyd-Smith et al. (2005), we implement the heterogeneity of the expected reproductive numbers by a Γ-distribution

$$Q(R_{\exp}; R_0, k) = \frac{(k(R_{\exp}/R_0))^k \, e^{-k(R_{\exp}/R_0)}}{R_{\exp}\Gamma(k)} \quad (5)$$

with mean R_0 and dispersion parameter k. The mean expected reproductive number R_0 in this model is equivalent to the basic reproductive number known from traditional epidemic models, and it shows the same threshold characteristics, with certain extinction of disease for values of $R_0 \leqslant 1$. For large values of the dispersion parameter k, the distribution is strongly peaked around R_0, with the homogeneous case arising in the limit of $k \to \infty$. When k is small the distribution is over-dispersed, with the majority of infective cases not contributing to further transmission in the epidemic at all. The special case of $k = 1$ yields an exponential distribution.

Using a Γ-distribution for the expected reproductive numbers, the offspring distribution given in Eq. (2) reduces to a negative binomial distribution given by

$$P(R_{\text{act}}; R_0, k) = \frac{\Gamma(R_{\text{act}} + k)}{\Gamma(R_{\text{act}} + 1)\Gamma(k)} \frac{k^k R_0^{R_{\text{act}}}}{(R_0 + k)^{R_{\text{act}}+k}} \quad (6)$$

which largely follows the shape of the underlying Γ-distribution, albeit defined on a discrete set. With this, the parameters of Eq. (4) are given as

$$\alpha = ((k/R_0 + 1)/(k + 1))[(k + R_0)/(k + 1)]^k \text{ and } B = k(k + R_0)^2/2\pi R_0^2(k + 1)^3.$$

For $R_0 = 1$ it follows that $\alpha = 1$, and the outbreak size distribution is a power law with exponent of $-3/2$, regardless of the level of dispersion, k. For any other values of R_0 the power law is modified by the exponential term α^{-s}. Integrating the outbreak size distribution to form the cumulative outbreak size distribution, i.e. the probability of observing an outbreak of size $s' \geqslant s$, then $P(s' \geqslant s) \sim s^{-1/2}$.

2.1. Outbreaks in an infinite population

To simulate an epidemic in this model, one individual is infected at time $t = 0$ in an otherwise totally susceptible population. From the time of infection, each case spends a fixed time in the infectious stage (I), before moving into the recovered class (R). For each new infection an individual expected reproductive number, $R_{i,\exp}$ is sampled, which in turn determines its transmission rate during the infectious stage. For the duration of infectiousness, the transmission rate is kept constant, and transmission events occur according to a time-inhomogeneous Poisson process with an intensity given by the sum of transmission rates of all currently infectious individuals. Simulations are run until the epidemic is finished (i.e. there are no infectious individuals in the population), or they reached a maximum number $s_{\max} = 25{,}000$ infections. The total epidemic size, s, is given by the number of recovered individuals at the end of an epidemic (for those epidemics that did not finish before reaching $s_{\max}$ infections, the total size is censored, we only know $s \geqslant s_{\max}$).

Fig. 1 shows the cumulative outbreak distributions for a variety of basic reproductive numbers R_0 and dispersion parameters k. The cumulative distribution is frequently used to analyse epidemiological data (Jansen et al., 2003; Rhodes et al., 1997; Trottier and Philippe, 2005).

Some general features of these outbreak size distributions include the steep drop-off between outbreak sizes 1 and 2, which is seen for small k, i.e., large heterogeneity in transmission. This reflects the increasing probability that the primary case will not transmit at all as k decreases. Furthermore, for large outbreak sizes s the curves converge to the invasion probability of the associated branching process, which is 0 for values of $R_0 \leqslant 1$, and positive for larger values of R_0. Irrespective of the degree of heterogeneity of transmission, $R_0 = 1$ remains an indicator of the threshold for establishment of the disease in the population.

For $R_0 = 1$ the cumulative outbreak size distribution gradients are $-1/2$ on the log–log scale, and independent of k for large s. This follows, as described above, from Eq. (4). For large k, the standard branching process result is recovered and as k decreases epidemics become increasingly hard to initiate, as the probability that the first case will transmit at all decreases.

When $R_0 < 1$, for large k, the outbreak size distribution follows that of a standard branching process with homogeneous transmission, and the absolute value of the gradient of the distribution is $> 1/2$, as expected. Outbreaks in this parameter region exhibit a similar pattern to observed measles outbreaks in highly vaccinated populations, such as England and Wales (Jansen et al., 2003). (There an increase in R was observed as vaccination rates declined.) As k decreases (i.e. as the degree of superspreading increases), there is the emergence of a well-defined scaling region (i.e. region of linearity in a log–log plot) in the distribution and, for small outbreak sizes, the absolute value of the gradient goes $< 1/2$. This has not been seen in other branching process models, and is reminiscent of the outbreak size distributions seen in isolated island data (Rhodes and Anderson, 1996; Rhodes et al., 1997). A more detailed quantitative comparison with empirical data is presented in Section 3. More generally, the effect of increasing heterogeneity in transmission is to generate epidemic outbreak distributions that appear to result from a higher R_0 than is actually the case, as the larger epidemics become correspondingly more frequent. Also visible from Fig. 1 is the tendency noted by Lloyd-Smith et al. (2005) for increasing heterogeneity to inhibit epidemic outbreaks; specifically the frequency of small outbreaks is diminished as k decreases. However, this is balanced by an increased frequency of larger epidemics over and above that expected from homogeneous transmission. Therefore, if there is significant heterogeneity in the transmission of a communicable disease it is more difficult for the disease to invade the population, but if it does succeed there is increased risk of larger epidemics.

For $R_0 > 1$ it is apparent that as k gets smaller there is less dependence upon R_0 as a determinant of the epidemic dynamics. The same calculations for larger values of R_0 give similar results (not shown). If superspreading is a significant characteristic of disease spread then similar patterns of observed outbreak sizes could arise from widely differing reproductive numbers. However, we *would* expect epidemic curves to reflect the underlying reproductive number after the early stages, if the population is big enough to sustain a large outbreak. While it is difficult to diagnose the reproductive number if there is large heterogeneity in transmission, it still is a threshold quantity for disease establishment, and therefore important when quantifying the strength of necessary control measures. Lloyd-Smith et al. (2005) report k values predominantly in the range 0.1–1.0 for a variety of communicable diseases.

Also shown in Fig. 1 are the outbreak distributions calculated using Eq. (4). For large s, where the approximations made in the derivation are valid, these agree well with the simulations.

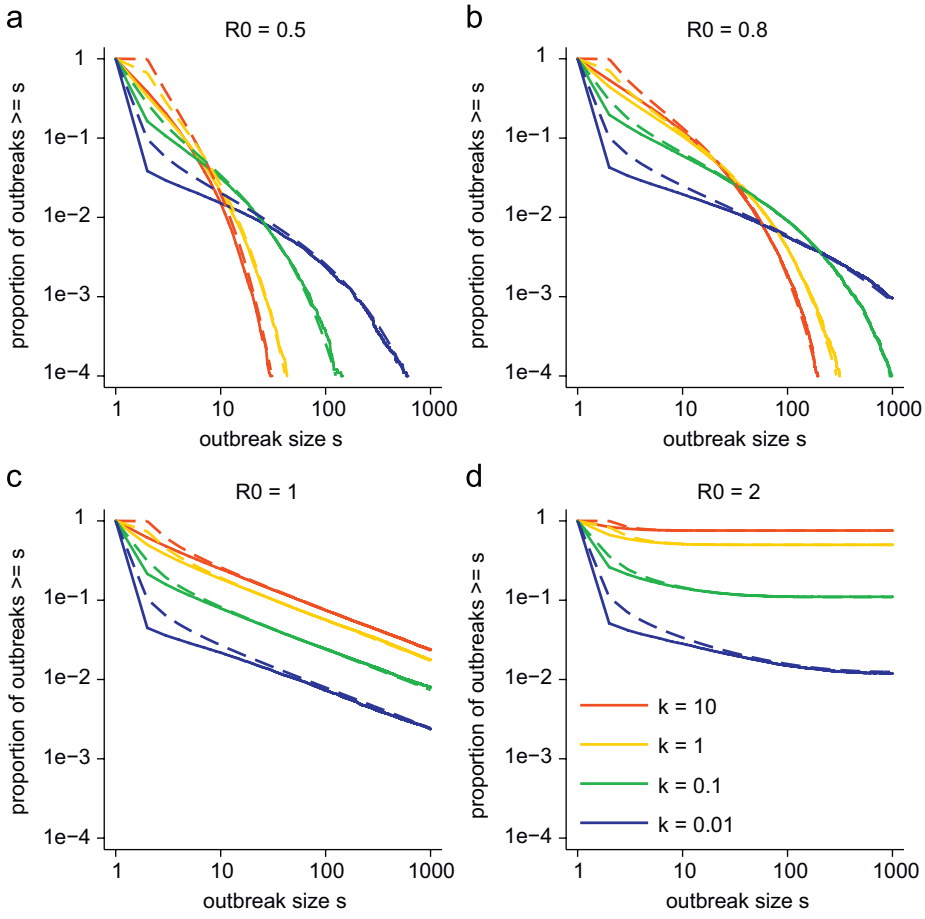

Fig. 1. Epidemic outbreak size distributions for $R_0 = 0.5$, $R_0 = 0.8$, $R_0 = 1$ and $R_0 = 2$. The values of dispersion to reflect changing levels of heterogeneity are $k = 10$, 1, 0.1 and 0.01. Solid lines show the cumulative outbreak size distributions obtained from 100,000 simulated epidemics per parameter combination; dashed lines show the analytic approximation given in Eq. (4).

2.2. Outbreaks in a finite population

While in an infinite population the proportion of susceptibles is unity throughout the epidemic, the depletion of susceptibles becomes an issue in finite populations. In the later stages of an epidemic in a finite population, transmission is reduced as the proportion of susceptibles, and therefore the probability that any contact is with a susceptible, decreases as the epidemic goes on. In practice, a finite population size is implemented by modifying the transmission rate β of any infectious individual by the proportion of susceptibles, (S/N), at any time throughout the epidemic to yield an effective transmission rate $\beta_{\text{eff}}(t) = (S(t)/N)\beta$. Due to the limited supply of susceptibles in a finite population, there is the potential to curtail the largest (though less frequent) epidemics. Fig. 2 shows the simulation results for $R_0 = 0.8$ in a population of 10,000. The finite population size diminishes the frequency of larger epidemics, particularly at small values of k. For larger values of R_0 the lack of susceptibles only becomes apparent for outbreak sizes very close to the population size, resulting in a steep cut-off (results not shown).

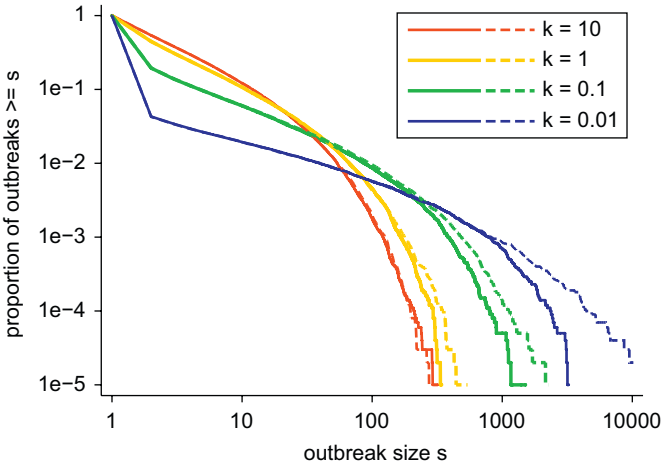

Fig. 2. Epidemic outbreak size distribution for $R_0 = 0.8$ in a population of size 10,000 compared to those for an infinite population. Solid lines show the simulation results for the finite population, obtained from 100,000 simulations per parameter set, dashed lines are the corresponding simulation results (from Fig. 1) for an infinite population.

3. Extended epidemiological model

The results presented above indicate that heterogeneous transmission can have a significant impact on observed patterns of communicable disease outbreaks. The source of this heterogeneity may be due to many factors, such as asymptomatic infection, increased social interaction during the infectious period, self-imposed isolation by some during infection, or greater or lesser viral shedding depending upon host immune status, and there may be others. The model cannot discriminate between

these possibilities; rather it can help to identify those situations where some form of heterogeneity in transmission may have occurred. In this section, we compare the results of a generalised superspreading model with some empirical data.

3.1. Data

Isolated island populations have often served as useful subjects of study in both epidemiological and ecological research. Detailed, accurate and long-running data exists for communicable disease in the Faroe Islands. Before the implementation of mass-vaccination, the infrequent introduction of infection from outside the islands led to a historical sequence of epidemics of varying sizes. Due to the small size of the population ($\sim$25,000) disease epidemics invariably died out after a period of weeks, only to re-emerge after the arrival of an index case from an outside reservoir (usually the United Kingdom and mainland Europe). In what follows we consider pre-mass-vaccination measles epidemics in the period 1910–1969.

Additionally, there are data collected from the on-going communicable disease monitoring programme in the United Kingdom. Of particular interest are data relating to outbreaks of measles in populations with high (but declining) vaccine uptake. Concentrations of susceptibles have been aggregating (particularly in large urban centres) due to reluctance to vaccinate pre-school children with the triple measles, mumps and rubella (MMR) vaccine. As a consequence, epidemics of measles are triggered by the arrival of index cases (Jansen et al., 2003).

Previous analysis of island disease data has shown the existence of a power-law scaling in the outbreak size distributions for measles and a number of other common communicable diseases. This pattern has been observed in several island populations (Rhodes and Anderson, 1996) and for communicable disease data in Canada (Trottier and Philippe, 2005). One of the particularly striking features of the results is the similarity of the exponents across different island communities. Conventional epidemic models have been unable to replicate the behaviour and hitherto only spatially explicit individual-based lattice models have been shown to reproduce the exponent (Rhodes and Anderson, 1996). By contrast, the pattern of recent measles outbreaks in England and Wales has been addressed by a standard branching process model (Jansen et al., 2003).

3.2. Extended model

Here, we examine whether a branching process model that admits the possibility of heterogeneous transmission of disease may give some insight into the patterns of epidemic outbreaks. The results from the calculations above suggest that significant heterogeneity tends to dominate effects due to R_0. The epidemiological model presented above is now extended to include births and deaths in the population, and to consider the immunity in the population that remains after a previous outbreak.

While in the previous sections every epidemic started with a fully susceptible population, in the case of measles in unvaccinated populations (such as the Faroe Islands population in the 20th century), individuals acquire immunity after infection, and reduce the pool of susceptibles at the start of the next epidemic. The susceptibles are replenished slowly through the natural birth process. In highly vaccinated populations (such as the England and Wales measles dataset), immunity comes from the high coverage of MMR vaccination. However, the effect is similar to that of acquired immunity through previous infection, and new susceptibles are pooled by births. It is possible that these two distinct mechanisms driving immunity might lead to different patterns in the availability of susceptibles, but further investigation on that detailed point would be needed.

If only a proportion p of the population is susceptible at the start of an epidemic, this effectively reduces the population size to $N_{\text{eff}} = pN$ (this will of course vary between subsequent outbreaks). Furthermore, the effective transmission rate is reduced to $\beta_{\text{eff}} = p\beta$, as only a proportion p of contacts made are with a susceptible individual. Therefore, the effective reproductive number $R = pR_0$ at the start of the epidemic takes the place of the basic reproductive number R_0.

To match the demographics of the Faroe Islands, the population size is set to 25,000 with a life expectancy of 70 years and the birth rate is set to match the death rate to ensure a constant population size. Occasional (Poisson) introduction of infectives is used to initiate epidemics at an introduction rate of 2 per year. Whereas for the results presented in Section 2, each epidemic started in a fully susceptible population, we now track the number of susceptibles left at the end of an outbreak. During the inter-epidemic period, the susceptibles slowly replenish due to the birth–death process that replaces immunes (or susceptibles) by susceptibles. However, for these repeated epidemics, the proportion of susceptibles is already reduced at the start of an epidemic, depending on the level of immunity at the end of the previous epidemic and the inter-epidemic duration, leading to outbreak size distributions that are comparable to those of outbreak simulations started in a fully susceptible population, albeit with an R_0 similar to the mean R at the start of the repeated outbreaks.

As the combined population of England and Wales is around 50 million, it is not feasible to simulate repeated outbreaks in this population. However, the outbreak size distributions of repeated outbreaks in a population of 1 million are very similar to those obtained by independent outbreaks in an infinite population over the range of sizes that occur in the datasets, as long as the reproductive number is adjusted to take into account the immunity in the population. Therefore, England and Wales datasets were fitted to outbreak size distributions from an infinite population, and the low value of the reproductive number (for measles the basic reproductive number is thought to be in the region of 15–20; Anderson and May, 1991) reflects the immunity in the population, which mostly stems from vaccination.

Fig. 3 shows the outbreak size distribution for the extended superspreading model, with a mean importation rate of 2 infectives per year for a number of different R_0 and k values. As heterogeneity becomes more pronounced there is the emergence of a scaling region, and for $R_0 > 1$ the gradient of this scaling is $< 1/2$. The scaling law for the measles data in the Faroe Islands gives $N(>s) \propto s^{-\alpha}$ where $\alpha \simeq 0.25$ (Rhodes and Anderson, 1996), so the simulations suggest that a very high degree of heterogeneity may be responsible for the observed scaling in the empirical data, specifically the parameter region $k \sim 0.01$ with $R_0 \sim 1$ looks a promising place to begin comparing the model with data. The fit of the model to the data is explored in more detail below.

3.3. Data analysis

In order to analyse the degree of heterogeneity in transmission that might underlie the measles outbreaks in the England and Wales and Faroe datasets, we fitted the observed outbreak size distributions to a straight line in the log–log plot, with gradients shown in Table 1. Note that we excluded epidemics of size 1 from the analyses, as these are almost certainly under-reported, however it is unclear by how much. We ran simulations matching the demographics of the three datasets, sampling the (R,k)-space extensively with Latin-Hypercube sampling. For a preliminary scan of the parameter space, we considered values of

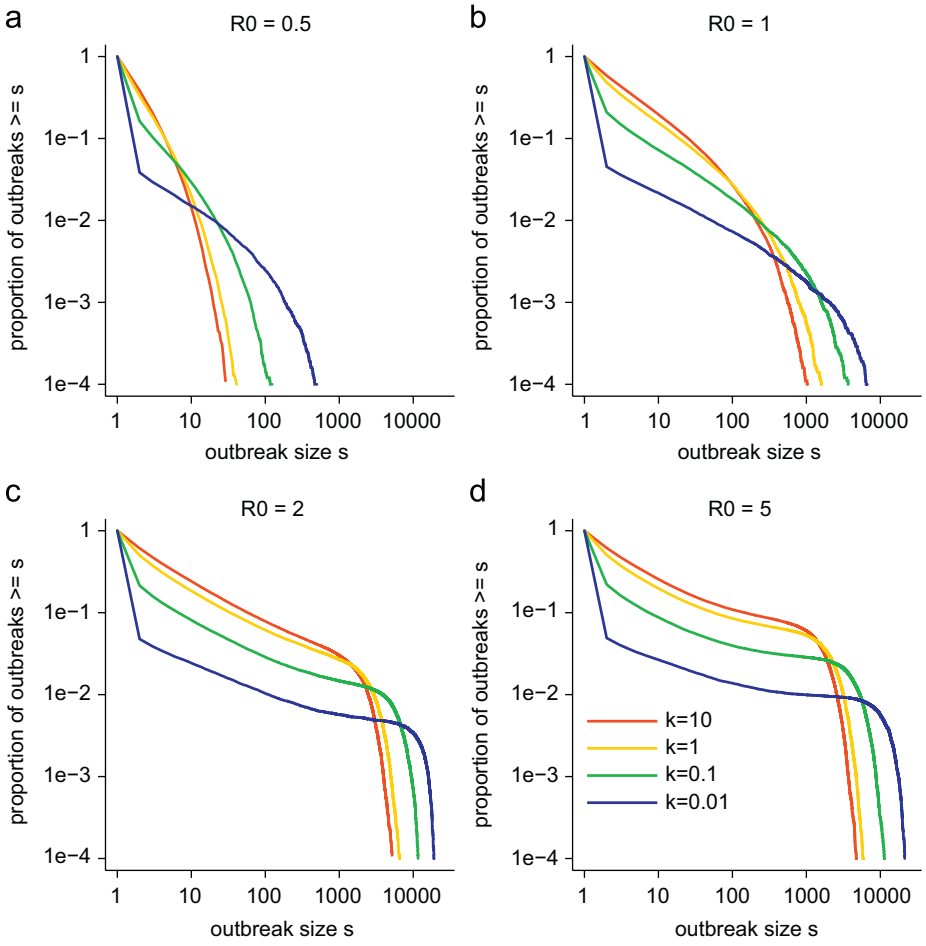

Fig. 3. Simulated epidemic outbreak size distribution for measles in a population of 25,000 for several basic reproductive numbers R_0 and varying degrees of heterogeneity of transmission k, obtained from 100,000 simulated epidemics per parameter combination. Infectives were introduced into the population twice a year on average.

Table 1
Gradients and 95% CI of the log–log outbreak size distributions for the different datasets, and the range of the outbreak sizes included in the analysis

Dataset	Gradient (95% CI)	Outbreak sizes included
England/Wales 1995–1998	−2.0 (−2.5 to −1.4)	2–10
England/Wales 1999–2002	−0.9 (−1.0 to −0.8)	2–100
Faroe	−0.25 (−0.26 to −0.24)	2–1000

$R = 10^{-2} \cdots 100$ and $k = 10^{-5} \cdots 100$, however, the data shown in Fig. 4 was obtained from a sample of 40,000 (R,k) parameter sets with $R = 10^{-2} \cdots 10$ and $k = 10^{-4} \cdots 10$, sampled on the log scale. For each (R,k) parameter set, 10,000 epidemics were simulated to generate the outbreak size distribution, and a straight line was fitted through the log–log transformed distribution over the same range as that of the dataset. Any datasets that yielded a good fit to the straight line (with a goodness-of-fit parameter of 0.98 or higher), and fell within the 95% CI of the gradient of the dataset was deemed consistent with the data. These consistent parameter values are plotted in Fig. 4. Note that Fig. 4 shows the effective reproductive number R (as described in Section 3.2).

The England and Wales measles datasets are compatible with a range of R and k values, and it is not possible to diagnose the underlying heterogeneity of transmission from the outbreak size distributions alone, however, they occupy distinct regions of the parameter space. Comparing the datasets of England and Wales with each other, it is likely that there was similar

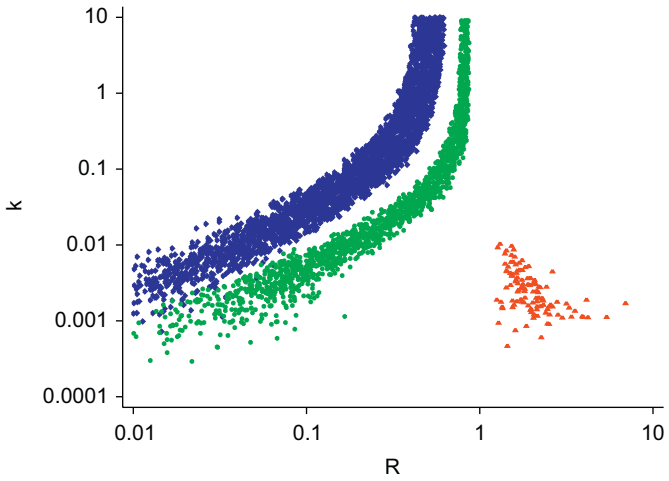

Fig. 4. Combinations of (R,k)-parameter values that are consistent at the 95% confidence level with the gradients of the log-log outbreak size distributions observed in the datasets. England and Wales 1995–1998—blue diamonds, England and Wales 1999–2002—green circles, Faroe 1910–1969—red triangles.

heterogeneity in transmission over the two time-periods considered, with lower values of the reproductive number R for higher heterogeneity. However, the value of R has increased markedly from 1995–1998 to 1999–2002, presumably as a result of the lower vaccination rates following the MMR vaccine scare

(Jansen et al., 2003). However, for both datasets R is still below 1, so the vaccine coverage is still sufficient to ensure control.

The situation for the Faroe Islands is different, with $R>1$ predicted for nearly all parameter combinations consistent with the data. This goes in line with the situation where the disease dies out due to the depletion of susceptibles, with an effective R well below 1 at the end of the epidemic, and re-introduction of the disease occurs only once the susceptibles were replenished over and above the herd-immunity threshold, such that a major epidemic with a reproductive number above 1 at the start is possible again. However, the results suggest that there is a strong degree of heterogeneity in the Faroe Islands dataset, with $k<0.01$, which may reflect the response of the community to the presence of a potentially dangerous communicable disease.

4. Disease control in the presence of superspreading

The possibility of significant heterogeneity in disease transmission has consequences for the design and implementation of intervention strategies. This has been demonstrated in macroparasitic diseases and sexually transmitted diseases (STDs) where the bulk of the transmission tends to be driven by a minority of the population (Anderson and May, 1991). Experience with these diseases suggests that some form of targeted vaccination strategy aimed at the likely superspreaders will be more effective than a standard uniform cross-population programme. The intention here is to investigate the impact of control strategies on the epidemic outbreak distribution. Specifically, we are interested in understanding how the pattern of epidemics triggered by the arrival of infection from outside the population is changed when that population is subject to various forms of intervention.

Following Lloyd-Smith et al. (2005), we suggest three different control strategies, all of which are parameterised by the control effort c:

(i) *Population-wide control (PWC):* Here the expected reproductive number of each case is reduced by a proportion c from R_{exp} to $(1-c)R_{\text{exp}}$. This is identical to reducing the mean R_0 to $(1-c)R_0$. This might for example be achieved by social distancing measures such as school and workplace closures that reduce the number of contacts for any individual in the general population, or by a population-wide administration of a vaccine that is not fully effective. Such a vaccine might be expected to be available in the early stages of an influenza pandemic.

(ii) *Random individual control (RIC):* Here a proportion c of the population is controlled perfectly, i.e., it has its expected reproductive number R_{exp} reduced to zero. This could be achieved by immunising a proportion of c individuals with a fully effective vaccine selected at random from the population. This is the foundation on which many immunisation strategies for communicable diseases are constructed.

(iii) *Targeted individual control (TIC):* This is an improvement on the random individual control in that the proportion c of the population containing the individuals with the highest expected reproductive numbers R_{exp} are chosen for control. (In the model, this is done by calculating the relevant percentile of the Γ-distribution and eliminating all cases with a higher R_{exp}.) This reflects the type of approach adopted in targeting immunisation at core groups in the spread of STDs, for example.

The aim of any control policy is firstly to try to attempt to prevent the establishment of endemic disease and secondly to reduce the size and frequency of the larger epidemics. Eradication can be achieved with certainty if the effective reproductive number under the control policy falls below 1. For both PWC and RIC, the basic reproductive number R_0 is reduced to $(1-c)R_0$ (see Lloyd-Smith et al., 2005, or Appendix A), yielding a critical control effort of $c_{\text{crit}} = 1 - 1/R_0$ for both strategies, as in classical epidemiological models without heterogeneity in transmission (Anderson and May, 1991).

If the control effort is insufficient to reduce the mean reproductive number below 1, there is however a finite chance that the epidemic will die out. This extinction probability is larger under RIC than under PWC if $c<c_{\text{crit}}$ (Lloyd-Smith et al., 2005). However, while for a sufficient control effort $c>c_{\text{crit}}$, extinction of the disease is certain, the proportion of large outbreaks is increased for RIC compared to PWC irrespective of individual variation in transmission, see our simulation results shown in Fig. 5. This also agrees with the predictions from branching process theory shown in Appendix B. These simulations use the simpler model as described in Section 2, with an infinite population. The population is assumed 100% susceptible before the implementation of the control strategy. The index case is introduced into the population subject to control measures.

Considering the individual-based control, the effectiveness of the control can be improved dramatically by targeting the part of the population that is likely to transmit the most, if these can be identified a priori. Although the TIC strategy implementing perfect targeting is unlikely to be realised in practice, this scenario highlights the potential gain in effectiveness that could theoretically be achieved by perfect targeting. Fig. 6 shows the effect that perfect targeting has on the effective reproductive number compared to the RIC strategy for various values of the control effort c and the dispersion parameter k (see Appendix B for further details). The effect of targeting becomes more pronounced as the heterogeneity in transmission increases: although the same proportion of the population is under control measures, with more heterogeneity the most infectious proportion accounts for a larger proportion of the transmission.

5. Conclusions

Whilst much attention has been paid to the effects of age-structure or the spatial distribution of a population upon communicable disease dynamics, significant levels of heterogeneity in disease transmission have not, until the work of Lloyd-Smith et al. (2005), been considered in epidemic modelling. Given the perceived threat of emerging strains of new infectious agents it is important to gain an insight into how heterogeneity of transmission may be made manifest in observed data.

Here, we have shown that such heterogeneity can have a significant effect on useful measures of disease status, such as the outbreak size distribution. Specifically, we have shown that heterogeneity can inhibit the establishment of disease in a population but, once present, can generate an excess of large epidemics over what would be expected using homogeneous assumptions. Additionally, the value of basic reproductive number as a guiding metric for the likely impact of a disease is shown to be somewhat diminished as heterogeneity increases. Also care must be exercised in interpreting outbreak size distributions as a guide to estimating the likely reproductive number of a disease. The results of this paper suggest that scaling in epidemic outbreak distributions (Rhodes et al., 1997; Trottier and Philippe, 2005) can arise when epidemics are driven by a small proportion of the population, with most infectives failing to go on to infect others.

The impact of three different disease control strategies has been investigated. The effectiveness of the control strategies depends upon the level of control that is available and the degree

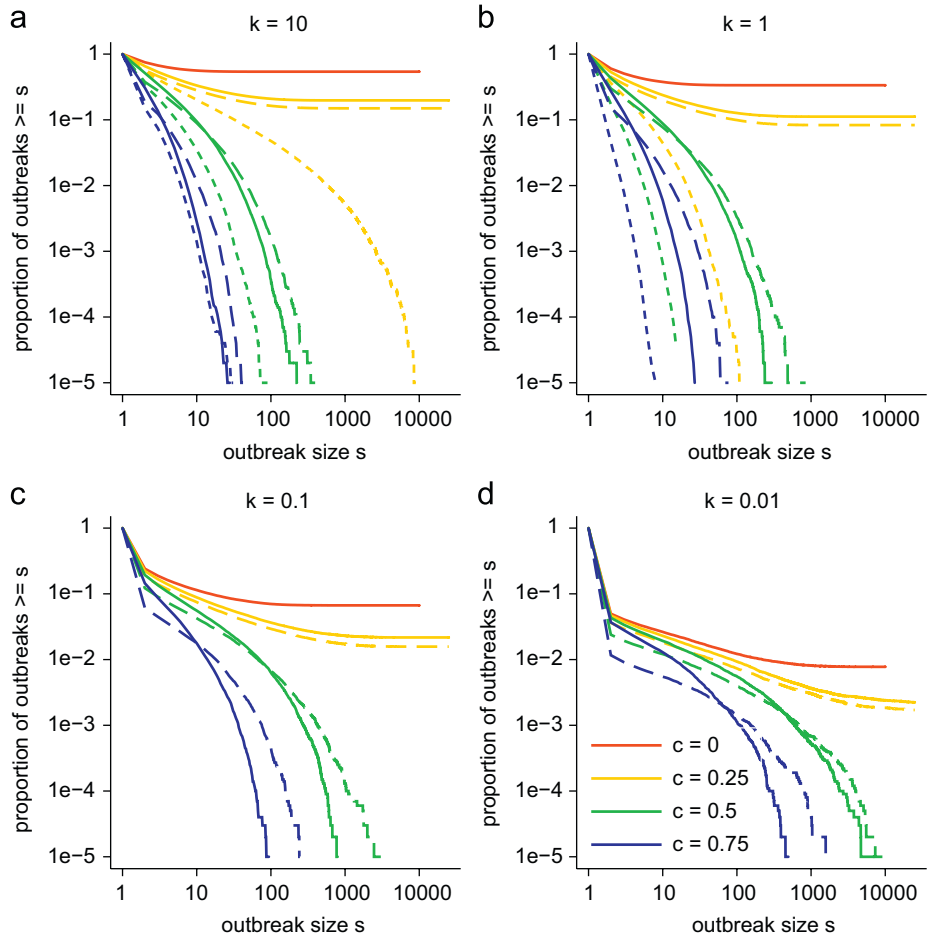

Fig. 5. Effect of intervention on outbreak size distributions. Simulation results for a disease with $R_0 = 1.5$ for four different levels of superspreading ($k = 10, 1, 0.1, 0.01$). Control at three different levels is shown $c = 0.25$, 0.5 and 0.75. Solid lines show population-wide control, dashed lines individual random control, short dashed lines targeted individual control. Note that for $k < 1$, none of the 100,000 simulated outbreaks per control effort showed any transmission and subsequent epidemic for targeted individual control.

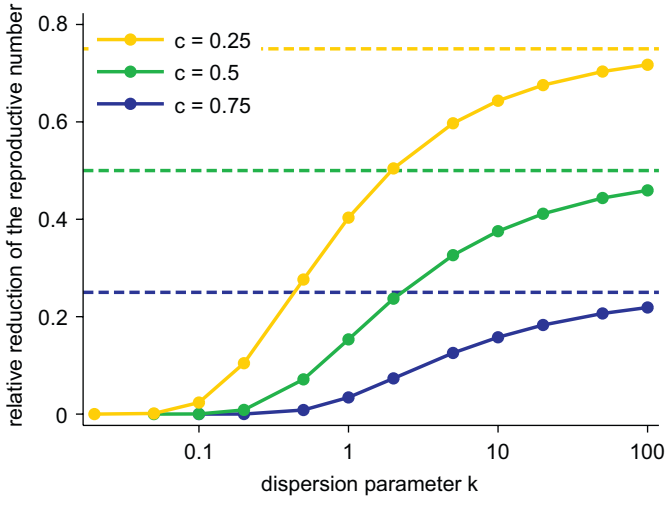

Fig. 6. Effect of targeting individual controls to the most infectious proportion c of the population, depending on the level of heterogeneity in transmission for control efforts $c = 0.25$, 0.5, 0.75. Random controls are equivalent to targeted controls in a population with homogeneous transmission.

of heterogeneity of transmission. Population-wide and random individual control policies yield similar results if applied with the same control effort, and in particular the effective reproductive number under control is identical for both cases, and independent of the amount of heterogeneity of transmission. If control cannot be achieved, the probability of stochastic extinction is slightly higher under random individual control, whereas in case of successful containment, population-wide control leads to smaller outbreak sizes. Using a control approach targeted at the most infectious individuals improves efficiency of controls massively, if the heterogeneity of transmission is large.

In the course of the analysis attention has been drawn to the patterns of outbreaks of measles in a highly vaccinated population (England and Wales, late 20th century) and pre-vaccination isolated island data (Faroe Islands, 20th century). While both settings are consistent with a range of heterogeneity in transmission, they differ in the inter-relation between the dispersion parameter k and the reproductive number R. For the England and Wales setting, large heterogeneity in transmission would imply very small values of R (smaller than expected from the vaccination coverage and basic reproductive number) therefore indicating that more homogeneous transmission is more likely. In the Faroe Islands setting, however, the correlation between reproductive number and dispersion parameter is weaker, indicating that a large degree of heterogeneity in transmission is consistent with the data.

It is possible that rather than differences in the pathology of the disease within hosts there may be a difference in the way the respective communities have reacted to the presence of disease.

In the early 20th century the occurrence of large-scale measles infection in subsistence communities, such as the Faroe Islands, had a very significant impact. It was regarded as a serious (and potentially fatal) disease. The simulations above indicate that much of the transmission in many epidemics might have been driven by a small proportion of those infected. Most infectives, therefore, might not go on to infect others suggesting a strong degree of self-imposed isolation by the majority of the cases.

By contrast, in the UK today there is less awareness of the presence and symptoms of measles, and infection is not viewed with the same seriousness. Therefore, identification of measles generally occurs later in the infectious period, thereby allowing significant time for the host to maintain normal patterns of circulation. Consequently the epidemic patterns will be consistent with well-mixed homogeneous models. These two differing epidemic outbreak patterns illustrate that information about disease and its prevalence in a population might have significant effects on the pattern of propagation, and it is an issue that needs further scrutiny (Jansen, private communication).

It has been observed that large heterogeneity in transmission leads to explosive epidemic curves (Lloyd-Smith et al., 2005), thereby making containment in the early stages of an epidemic more difficult. However, the model used there uses discrete generations and, as a consequence, will not reproduce realistic epidemic curves, particularly on short timescales. Our implementation as a continuous-time Markov process gives access to somewhat more realistic epidemic curves. It will be very interesting to investigate patterns in these epidemic curves. If heterogeneity in transmission does indeed lead to different epidemic curves than those observed in homogeneous models, this might give early insight into the amount of heterogeneity when faced with novel emergent diseases (such as SARS or species jumping influenza) and may ultimately help with choosing the best control strategies. Future work will investigate this possibility.

In the analysis of STDs, classical homogeneous mixing models have failed to reproduce observed epidemic patterns, promoting the use of network models, which capture the actual heterogeneity of society in terms of number of sexual contacts and mixing patterns better. However, as networks are very complicated structures, it will be useful to investigate how well the observed epidemic patterns can be reproduced by a simple model similar to the one used here, which allows for heterogeneity in transmission, but assumes homogeneous mixing patterns. Also, the investigation of extensions of the model to incorporate non-random mixing patterns could give useful insight.

Acknowledgements

TG and CJR are supported by IC-IMS and RCUK. We would like to thank two anonymous reviewers for their constructive comments which helped to improve the manuscript substantially. Furthermore, we thank the HPA for providing the UK measles data.

Appendix A. The superspreading model as a Galton–Watson process: approximating the outbreak size distribution

The continuous-time Markov chain model described in Section 2 is equivalent to a Galton–Watson branching process (Harris, 1963) when considering only the outbreak size distribution and not the time-course of epidemics. In this branching process, each case i infects $R_{i,\mathrm{act}}$ new cases with a probability given by the negative binomial offspring distribution (6).

For this offspring distribution, the generating function for this process is given by

$$f(w)=\sum_{i=0}^{\infty}P_i w^i=\left(1+\frac{R_0}{k}(1-w)\right)^{-k} \tag{A.1}$$

with $P_i=P(R_{\mathrm{act}}=i;R_0,k)$from Eq. (6) (Lloyd-Smith et al., 2005).

The probability that no transmission takes place after the index case is introduced into the population (yielding an outbreak of size 1) is given by P_0, whereas the probability of extinction, q (i.e. the probability of observing a finite outbreak size) is given by the solution of $f(q)=q$. These asymptotics agree well with the simulation results.

The outbreak size can be described by a branching process with generating function

$$F(w)=wf[F(w)]. \tag{A.2}$$

For $R_0>1$, the mean outbreak size μ diverges, however, in the case of $R_0\leqslant 1$, extinction is certain, and the mean outbreak size μ is given by

$$\mu=\frac{1}{1-R_0}, \tag{A.3}$$

independently of the value of k (Haccou et al., 2005).

Following Otter (1949) (see also Harris, 1963), the outbreak size distribution of a Galton–Watson branching process can be approximated for large outbreak sizes s, by the Lagrange equation given in Eq. (4) with

$$B=\frac{a}{2\pi\alpha f''(a)}, \tag{A.4}$$

where a is given as the solution to $a=f(a)f'(a)$, and $\alpha=a/f(a)$.

For the negative binomial offspring distribution with generating function (A.1) we have

$$f'(w)=\left(\frac{1}{R_0}+\frac{1-w}{k}\right)^{-1}f(w), \tag{A.5}$$

$$f''(w)=\left(1+\frac{1}{k}\right)\left(\frac{1}{R_0}+\frac{1-w}{k}\right)^{-2}f(w), \tag{A.6}$$

and thus

$$a=\frac{k/R_0+1}{k+1}. \tag{A.7}$$

With this

$$\alpha=\frac{a}{f(a)}=\frac{k/R_0+1}{k+1}\left(\frac{k+R_0}{k+1}\right)^{k}, \tag{A.8}$$

and

$$B=\frac{k(k+R_0)^2}{2\pi R_0^2(k+1)^3}, \tag{A.9}$$

as given in the main text.

The cumulative outbreak size distributions shown in Fig. 1 are obtained by summing over the probabilities of observing an outbreak of size $s'\geqslant s$,

$$P(s'\geqslant s)=\sum_{s'=s}^{\infty}P(s'). \tag{A.10}$$

Appendix B. Outbreak sizes in the presence of controls

In the presence of controls, Eq. (4) is still valid. However, as the controls change the offspring distribution, this also affects the particular form of α and B.

B.1. Population-wide control

For population-wide control (PWC) with control effort c, the expected reproductive number of each case is reduced from R_{exp} to $(1-c)R_{\text{exp}}$. This still leads to a negative binomial offspring distribution but with R_0 replaced by $(1-c)R_0$ in Eq. (6). Therefore, the outbreak size distribution for the population-wide control policy has the same functional form as the outbreak size distribution in the absence of controls, with a reduced $R_{0,\text{PWC}} = (1-c)R_0$.

B.2. Random individual control

For random individual control (RIC) with control effort c, a proportion of the population is controlled perfectly; therefore the offspring distribution is given by

$$P_{i,\text{RIC}} = \begin{cases} c + (1-c)P_0 & \text{if } i = 0, \\ (1-c)P_i & \text{otherwise,} \end{cases} \tag{B.1}$$

with P_i as above for the uncontrolled case. The effective reproductive number under control is given by

$$R_{0,\text{RIC}} = \sum_{i=0}^{\infty} i \times P_{i,\text{RIC}} = (1-c)\sum_{i=1}^{\infty} i \times P_i = (1-c)R_0, \tag{B.2}$$

as in the case of PWC.

The generating function is given by

$$f_{\text{TIC}}(w) = c + (1-c)f(w), \tag{B.3}$$

with derivatives $f'_{\text{RIC}}(w) = (1-c)f'(w)$ and $f''_{\text{RIC}}(w) = (1-c)f''(w)$. In contrast to the case of no controls there is no analytic expression for the point $a_{\text{RIC}} = f_{\text{RIC}}(a_{\text{RIC}})/f'_{\text{RIC}}(a_{\text{RIC}})$, and therefore for α and B. However, a numerical evaluation of a_{RIC} yields results for the outbreak size distributions that match the simulation results as well as in the no control case shown in Fig. 1 (results not shown).

B.3. Targeted individual control

For targeted individual control (TIC), a proportion, c, of the population is controlled perfectly. However, in this case it is that proportion with the largest expected reproductive number R_{exp}. This means that the distribution for the expected reproductive numbers which for the no controls case is assumed to be the Γ-distribution given in Eq. (5), is cut off at a critical value R_{crit} which is determined by the relevant percentile of the Γ-distribution as

$$G(R_{\text{crit}}) = \int_0^{R_{\text{crit}}} Q(R; R_0, k)\,\mathrm{d}R = 1 - c. \tag{B.4}$$

As the Γ-distribution has no analytic cumulative distribution function, this integral has to be evaluated numerically. However, due to the scaling of the Γ-distribution with R_0 we know that R_{crit}/R_0 is only a function of c and k, and independent of R_0.

With this cut off distribution for the expected reproductive numbers, the offspring distribution is no longer a negative binomial distribution, but is given by

$$P_{i,\text{TIC}} = \frac{k^k R_0^i}{\Gamma(i+1)\Gamma(k)} \int_0^{R_{\text{crit}}/R_0} z^{i+k-1}\, \mathrm{e}^{[-(R_0+k)z]}\,\mathrm{d}z \tag{B.5}$$

for which, again, there is no analytic solution.

This means that we cannot specify the generating function for this process and therefore calculate the approximation to the outbreak size distribution. However, in order to gauge the efficiency of the TIC compared to that of the RIC it is useful to compute the effective reproductive number for this control option, given by

$$R_{0,\text{TIC}} = \sum_{i=0}^{\infty} i \times P_{i,\text{TIC}}. \tag{B.6}$$

Similarly to the cut-off value R_{crit}, $R_{0,\text{TIC}}/R_0$ is numerically virtually independent of R_0, and effectively only a function of k and c.

References

Anderson, R.M., May, R.M., 1991. Infectious Diseases of Humans: Dynamics and Control. Oxford University Press, Oxford.

Becker, N., 1974. On parametric estimation for mortal branching processes. Biometrica 61, 393–399.

Chen, M.I.C., Chow, A.L.P., Earnest, A., Leong, H.N., Leo, Y.S., 2006. Clinical and epidemiological predictors of transmission in severe acute respiratory syndrome (SARS). BMC Infect. Dis., 6.

Farrington, C.P., Kanaan, M.N., Gay, N.J., 2003. Branching process models for surveillance of infectious diseases controlled by mass vaccination. Biostatistics 4, 279–295.

Ferguson, N.M., Donnelly, C.A., Anderson, R.M., 2001. The foot-and-mouth epidemic in Great Britain: pattern of spread and impact of interventions. Science 292, 1155–1160.

Galvani, A.P., 2003. Immunity, antigenic heterogeneity, and aggregation of helminth parasites. J. Parasitol. 89, 232–241.

Grenfell, B.T., Wilson, K., Isham, V.S., Boyd, H.E.G., Dietz, K., 1995. Modelling patterns of parasite aggregation in natural populations: trichostrongylid nematode–ruminant interactions as a case study. Parasitology 111, S135–S151.

Haccou, P., Jagers, P., Vatutin, V.A., 2005. Branching Processes: Variation, Growth and Extinction of Populations. Cambridge University Press, Cambridge.

Harris, T.E., 1963. The Theory of Branching Processes. Springer, Berlin.

Hethcote, H.W., Yorke, J.A., 1984. Gonorrhea Transmission Dynamics and Control. Springer, Berlin.

James, A., Pitchford, J.W., Plank, M.J., 2007. An event-based model of superspreading in epidemics. Proc. R. Soc. B—Biol. Sci. 274, 741–747.

Jansen, V.A.A., Stollenwerk, N., 2005. Modeling measles outbreaks. In: Haccou, P., et al. (Eds.), Branching Processes: Variation, Growth, and Extinction of Populations. Cambridge University Press, pp. 236–249.

Jansen, V.A.A., Stollenwerk, N., Jensen, H.J., Ramsay, M.E., Edmunds, W.J., Rhodes, C.J., 2003. Measles outbreaks in a population with declining vaccine uptake. Science 301, 804.

Kiss, I.Z., Green, D.M., Kao, R.R., 2006. The network of sheep movements within Great Britain: network properties and their implications for infectious disease spread. J. R. Soc. Interface 3, 669–677.

Lipsitch, M., Cohen, T., Cooper, B., Robins, J.M., Ma, S., James, L., Gopalakrishna, G., Chew, S.K., Tan, C.C., Samore, M.H., Fisman, D., Murray, M., 2003. Transmission dynamics and control of severe acute respiratory syndrome. Science 300, 1966–1970.

Lloyd-Smith, J.O., Schreiber, S.J., Kopp, P.E., Getz, W.M., 2005. Superspreading and the effect of individual variation on disease emergence. Nature 438, 355–359.

Matthews, L., Woolhouse, M., 2005. New approaches to quantifying the spread of infection. Nat. Rev. Microbiol. 3, 529–536.

Matthews, L., Low, J.C., Gally, D.L., Pearce, M.C., Mellor, D.J., Heesterbeek, J.A.P., Chase-Topping, M., Naylor, S.W., Shaw, D.J., Reid, S.W.J., Gunn, G.J., Woolhouse, M.E.J., 2006. Heterogeneous shedding of *Escherichia coli* O157 in cattle and its implications for control. Proc. Natl. Acad. Sci. USA 103, 547–552.

May, R.M., Anderson, R.M., 1987. Transmission dynamics of HIV-infection. Nature 326, 137–142.

Otter, R., 1949. The multiplicative process. Ann. Math. Stat. 20, 206–224.

Rhodes, C.J., Anderson, R.M., 1996. Power laws governing epidemics in isolated populations. Nature 381, 600–602.

Rhodes, C.J., Jensen, H.J., Anderson, R.M., 1997. On the critical behaviour of simple epidemics. Proc. R. Soc. Lond. Ser. B—Biol. Sci. 264, 1639–1646.

Sguanci, L., Lio, P., Bagnoli, F., 2006. The influence of risk perception in epidemics: a cellular agent model. Cell. Autom. Proc. 4173, 321–329.

Trottier, H., Philippe, P., 2005. Scaling properties of childhood infectious diseases epidemics before and after mass vaccination in Canada. J. Theor. Biol. 235, 326–337.

Truscott, J., Garske, T., Chis-Ster, I., Guitian, J., Pfeiffer, D., Snow, L., Wilesmith, J., Ferguson, N.M., Ghani, A.C., 2007. Control of a highly pathogenic H5N1 avian influenza outbreak in the GB poultry flock. Proc. R. Soc. B 274, 2287–2295.

Woolhouse, M.E.J., Dye, C., Etard, J.F., Smith, T., Charlwood, J.D., Garnett, G.P., Hagan, P., Hii, J.L.K., Ndhlovu, P.D., Quinnell, R.J., Watts, C.H., Chandiwana, S.K., Anderson, R.M., 1997. Heterogeneities in the transmission of infectious agents: implications for the design of control programs. Proc. Natl. Acad. Sci. USA 94, 338–342.

Woolhouse, M.E.J., Shaw, D.J., Matthews, L., Liu, W.C., Mellor, D.J., Thomas, M.R., 2005. Epidemiological implications of the contact network structure for cattle farms and the 20–80 rule. Biol. Lett. 1, 350–352.